AMIR-HOMAYOON NAJMI

THE WIGNER DISTRIBUTION: A TIME-FREQUENCY ANALYSIS TOOL

Time-frequency distributions are enormously powerful tools for analysis of time series data. Often our data contain signals whose frequency content may be changing with time. Capturing this change with good frequency and time resolutions has been the subject of much research in the last two decades. The Wigner distribution and the associated Cohen class of generalized Wigner distributions offer a possible way to conduct such analysis. In this article I review some of the basic features of the Wigner distribution and emphasize its relationship to the two-dimensional ambiguity function. I discuss the interference terms that arise in the Wigner distribution of multicomponent signals and define the two most popular classes of kernal functions designed to eliminate cross-term interference. I point out that experimental kernel functions must be designed in the Doppler-lag domain with a complete knowledge of the signals of interest and give an example of an unusual kernel in one application. I apply the methods outlined to two real data sets obtained by APL staff during different experiments. For both sets, the Wigner distribution with appropriate kernel functions is shown to be superior to the standard spectrogram.

INTRODUCTION

Time-frequency analysis is one of the most important areas of signal processing. The standard Fourier analysis, although very useful in identifying individual frequency components of a signal, has no time resolution. Hence, efforts have continued in the last several decades to invent new methods for the analysis of local time and frequency content of waveforms.

The simplest of these methods is the short-time Fourier transform, i.e., the spectrogram, in which one transforms windowed sections of the data to the frequency domain. Time resolution is arrived at by centering the window function on the epoch of interest and then sliding the window along the time axis. Thus, one may obtain a time-frequency "image" that can serve as a useful tool in the analysis by delineating the frequency content of the signal as a function of time, much like a musical score denotes the individual tones in a piece as time progresses. Although this method is easy to implement and indeed is an indispensable analytical tool, it fails to provide high time and frequency resolution simultaneously. To localize some frequency component in time one must choose a very short window, which will inevitably lead to poor frequency resolution upon Fourier transformation. Conversely, to increase the frequency resolution one must Fourier-transform long sections of the data, which adversely affects the localization in time.

Notwithstanding its inherent resolution problems, the spectrogram has been successful in much data analysis, in part because most experimental data have temporal variations that are "slow." In some instances, the most notable being human speech, the time variations of the frequency content can be sufficiently fast to render the spectrogram practically useless.

Time-varying spectra were studied in the classical works of Gabor, Ville, Page, and Wigner. Their work was not motivated by improving on the spectrogram, but by a desire to construct a joint time and frequency distribution of energy of a waveform based on general mathematical principles. Wigner, of course, was concerned with constructing such a function for the quantum mechanical wavefunction, which, with its probabilistic interpretation, led naturally to the concept of a distribution function similar to those in probability theory.

In the rest of this article I shall describe the Wigner class of distributions and show how they are related to the two-dimensional ambiguity function. I shall describe how the so-called interference terms can be filtered in the ambiguity function space, give some examples of these distributions on synthetic data, and present two examples of an application to real data: data from an electromagnetic sensor and data from ocean current measurements taken during an internal wave experiment. Both data sets were obtained by APL staff.

THE WIGNER DISTRIBUTION

Consider a waveform $s(t)$. The instantaneous energy of the signal per unit time at time t is given by $|s(t)|^2$. The intensity per unit frequency is given by $|S(f)|^2$, where

$$S(f) = \int_{-\infty}^{\infty} s(t) e^{-2i\pi ft} \, dt$$

is the standard Fourier transform relationship. Parseval's theorem then states that the total energy can be computed in the time or the frequency domain; thus,

$$\int_{-\infty}^{\infty} |s(t)|^2 \, dt = \int_{-\infty}^{\infty} |S(f)|^2 \, df.$$

The fundamental goal is then to devise a joint function of time and frequency that represents the energy or intensity of a waveform per unit time and per unit frequency. This joint function, which we shall denote by $P(t,f)$, must necessarily satisfy the following "marginal" conditions:

$$\int_{-\infty}^{\infty} P(t,f) \, dt = |S(f)|^2$$

and

$$\int_{-\infty}^{\infty} P(t,f) \, df = |s(t)|^2.$$

The spectrogram is a time-frequency distribution and is defined as follows:

$$P_{\text{spectrogram}}(t,f) = \left| \int_{-\infty}^{\infty} s(\tau) w(\tau - t) e^{-2i\pi f \tau} \, d\tau \right|,$$

where the window function $w(\tau - t)$ is centered at time t.

The Wigner distribution for a real waveform $s(t)$ does satisfy the marginal properties (it is a quadratic functional of the signal) and is defined as follows:

$$P_{\text{wigner}}(t,f) = \int_{-\infty}^{\infty} \tilde{s}\left(t + \frac{\tau}{2}\right) \tilde{s}^*\left(t - \frac{\tau}{2}\right) e^{-2i\pi f \tau} \, d\tau,$$

where $\tilde{s}(t)$ is the so-called analytic signal whose imaginary part is related to the original waveform by Hilbert transformation; thus,

$$\tilde{s}(t) \equiv s(t) + i \frac{1}{\pi} \int_{-\infty}^{\infty} \frac{s(\xi)}{t - \xi} \, d\xi.$$

The analytic signal is used for several reasons. As is clear from its definition, the Wigner distribution is a quadratic functional of the signal and so it will, in general, exhibit interference between the negative and positive frequency components of the signal. However, if the analytic signal is used in the computation, no negative frequencies are present and hence no negative and positive frequency interference will persist. In addition, the analytic signal formulation guarantees that the first moment of the distribution is the instantaneous frequency, i.e., the time derivative of the signal phase function. As we shall see later, a practical algorithm for the computation of the Wigner distribution will have to rely on oversampling the original waveform to avoid serious aliasing in the frequency domain, *unless* the analytic signal formulation is used, in which case no oversampling is required. The following presents some properties of the Wigner distribution.[1,2]

- An alternative definition for the Wigner distribution can be given in the frequency domain:

$$P_{\text{wigner}}(t,f) = \int_{-\infty}^{\infty} \tilde{S}\left(f + \frac{v}{2}\right) \tilde{S}^*\left(f - \frac{v}{2}\right) e^{-2i\pi v t} \, dv,$$

where $\tilde{S}(f)$ denotes the Fourier transform of the analytic function $\tilde{s}(t)$.

- The marginal properties are satisfied:

$$\int_{-\infty}^{\infty} P_{\text{wigner}}(t,f) \, dt = \left| \tilde{S}(f) \right|^2,$$

$$\int_{-\infty}^{\infty} P_{\text{wigner}}(t,f) \, df = \left| \tilde{s}(t) \right|^2.$$

- The Wigner distribution is time-limited if the original waveform is time-limited, and frequency-limited if the original signal is frequency-limited.

- If $\tilde{s}(t) = \tilde{s}_1(t)\tilde{s}_2(t)$, then

$$P_{\text{wigner}}^s(t,f) = \int_{-\infty}^{\infty} P_{\text{wigner}}^{s_1}(t,v) P_{\text{wigner}}^{s_2}(t,f-v) \, dv.$$

Conversely, if $\tilde{s}(t) = \int_{-\infty}^{\infty} \tilde{s}_1(\tau)\tilde{s}_2(t-\tau) \, dt$, then

$$P_{\text{wigner}}^s(t,f) = \int_{-\infty}^{\infty} P_{\text{wigner}}^{s_1}(\tau,f) P_{\text{wigner}}^{s_2}(t-\tau,f) \, d\tau.$$
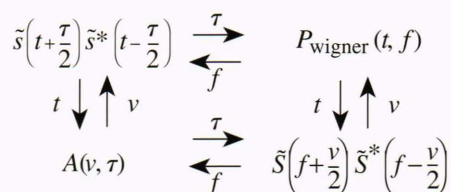
- The Wigner distribution and the two-dimensional ambiguity function are a Fourier transform pair. The two-dimensional ambiguity function is commonly used in radar signal analysis as the most complete statement of the waveform's inherent performance. It reveals the range-Doppler position of ambiguous responses and defines the range and Doppler resolution. It is defined as

$$A(v,\tau) \equiv \int_{-\infty}^{\infty} \tilde{s}\left(t + \frac{\tau}{2}\right) \tilde{s}^*\left(t - \frac{\tau}{2}\right) e^{2i\pi v t} \, dt.$$

The Fourier transform relationship is

$$P_{\text{wigner}}(t,f) \equiv \iint A(v,\tau) e^{-2i\pi v t - 2i\pi f \tau} \, dv \, d\tau.$$

- The following diagram can be constructed, where each arrow indicates a Fourier transformation on the indicated variable.[3]

$$
\begin{array}{ccc}
\tilde{s}\left(t+\frac{\tau}{2}\right)\tilde{s}^*\left(t-\frac{\tau}{2}\right) & \xrightarrow[f]{\tau} & P_{\text{wigner}}(t,f) \\[2mm]
t \downarrow \uparrow v & & t \downarrow \uparrow v \\[2mm]
A(v,\tau) & \xrightarrow[f]{\tau} & \tilde{S}\left(f+\frac{v}{2}\right)\tilde{S}^*\left(f-\frac{v}{2}\right)
\end{array}
$$

- The instantaneous frequency $\bar{f}_t$ is defined by

$$\bar{f}_t = \frac{\int P_{\text{wigner}}(t,f)f \, df}{\int P_{\text{wigner}}(t,f) \, df}.$$

Now, if we write the analytic signal in the form $\tilde{s}(t) = |\tilde{s}(t)| \exp[2i\pi\phi(t)]$, then the above equation reduces to the well-known relation $\bar{f}_t = \dot{\phi}(t)$.

- The "time center" at frequency f is analogously defined by

$$\bar{t}_f = \frac{\int P_{\text{wigner}}(t,f)t \, dt}{\int P_{\text{wigner}}(t,f) \, dt},$$

which is related to the derivative of the phase function of the Fourier transform function $\tilde{S}(f) = |\tilde{S}(f)| \exp[2i\pi\Phi(f)]$ through the analogous relation, viz. $\bar{t}_f = \Phi'(f)$. The latter can be interpreted as the group delay at frequency f of the waveform.

- The second moments of the Wigner distribution are somewhat less meaningful because the Wigner distribution itself is not positive-definite. For instance,

$$\sigma^2_{f|t} \equiv \overline{f_t^2} - \bar{f}_t^2 = -\frac{1}{2}\frac{d^2}{dt^2}\ln|\tilde{s}(t)|$$

is independent of the phase but is in general nonpositive! Thus, the second moment cannot be considered as a true variance.

- The most serious problem with the Wigner distribution is that it is a nonlinear functional of the original waveform. This has significant consequences on the output when the waveform is a sum of two or more independent components. Thus, if $s(t) = s_1(t) + s_2(t)$, then

$$P^s_{\text{wigner}} = P^{s_1}_{\text{wigner}} + P^{s_2}_{\text{wigner}} + P^{s_1 s_2}_{\text{wigner}} + P^{s_2 s_1}_{\text{wigner}},$$

where the cross-Wigner distribution is defined by

$$P^{s_1 s_2}_{\text{wigner}} = \int_{-\infty}^{\infty} \tilde{s}_1\left(t + \frac{\tau}{2}\right)\tilde{s}_2^*\left(t - \frac{\tau}{2}\right)e^{-2i\pi f\tau} d\tau.$$

The cross terms appearing in the Wigner distribution of multicomponent signals pose a serious problem, and for such signals (e.g., the sum of independent narrowband components), methods must be devised to minimize the contribution of the cross terms.

- A useful relationship that relates the Wigner distribution to the inner product of two signals and has applications in detection theory is Moyal's formula, which is basically a Parseval identity:

$$\left|\int_{-\infty}^{\infty} \tilde{s}_1(t)\tilde{s}_2^*(t) \, dt\right|^2 = \int\int_{-\infty}^{\infty} P^{s_1}_{\text{wigner}}(t,f)P^{s_2}_{\text{wigner}}(t,f) \, dt \, df.$$

To discretize the equation defining the Wigner distribution we begin with the ambiguity function and write it in the following equivalent form:

$$A(v,2\tau) \equiv \int_{-\infty}^{\infty} \tilde{s}(t+\tau)\tilde{s}^*(t-\tau)e^{2i\pi vt} \, dt.$$

Now we may discretize according to $t \to l\Delta T$ and $t \to n\Delta T$, where l and n are integers, and obtain

$$A(v,2l) = \Delta T \sum_{n=-\infty}^{\infty} s^*[n-l]s[n+l]e^{2i\pi vn\Delta T},$$

which gives the following equation for the Wigner distribution:

$$P_{\text{wigner}}[n\Delta T, f] = 2\int_{-\infty}^{\infty} \sum_{l=-\infty}^{\infty} A(v,2l)e^{-2i\pi vn\Delta T}e^{-4i\pi l\Delta Tf} \, dv.$$

For discrete frequencies we will clearly have frequency aliasing. To prevent this problem we can either oversample the input data by a factor of 2 or use the analytic signal. A discrete formulation of the latter can be given in terms of the following discrete Hilbert transformer:

$$H\{s[n]\} = \sum_{m \neq n} s[m]\frac{\sin^2\left[\pi\frac{m-n}{2}\right]}{\pi\frac{m-n}{2}},$$

which can be used in the construction of the analytic signal via $\tilde{s}[n] = s[n] + iH\{s[n]\}$.

THE COHEN CLASS OF TIME-FREQUENCY DISTRIBUTION FUNCTIONS

The relationship between the two-dimensional ambiguity function and the Wigner distribution can be generalized to define a wide class of time-frequency distributions.[2] Indeed, the Wigner distribution is a special case of a more general class of time-frequency functions parametrized by a two-dimensional kernel function K:

$$P_K(t,f) =$$
$$\int\int\int_{-\infty}^{\infty} \tilde{s}\left(u + \frac{\tau}{2}\right)\tilde{s}^*\left(u - \frac{\tau}{2}\right)K(v,\tau)e^{-2i\pi v(u-t)-2i\pi f\tau} \, du \, d\tau \, dv.$$

Clearly, the Wigner distribution is obtained by setting $K = 1$ in the above equation. The spectrogram is also a special case of that class and corresponds to the following choice of the kernel:

$$K_{\text{spectrogram}}(v,\tau) = \int_{-\infty}^{\infty} w\left(u - \frac{\tau}{2}\right)w\left(u + \frac{\tau}{2}\right)e^{-2i\pi vu} \, du.$$

To satisfy the marginal properties and ensure that the distribution is real, the kernel must satisfy the following: $K(v,0) = K(0,\tau) = 1$ and $K(v,\tau) = K^*(-v, -\tau)$.

Moyal's formula is no longer valid, but instead the following equation is true:

$$\left| \int_{-\infty}^{\infty} \tilde{s}_1(t)\tilde{s}_2^*(t)\,dt \right|^2 =$$

$$\int\int_{-\infty}^{\infty} P_{\text{wigner}}^{s_1}(t,f) P_{\text{wigner}}^{s_2}(t',f') Q(t-t',f-f')\,dt\,dt'\,df\,df',$$

where

$$Q(t,f) \equiv \int\int_{-\infty}^{\infty} |K(v,\tau)|^{-2}\, e^{2i\pi(vt+f\tau)}\,dv\,d\tau .$$

Thus, the strict Moyal formula is only valid when the kernel is identically unity. In general, the validity of Moyal's strict formula is not a requirement on the design of the kernel function.

The general relationship between the Wigner distribution and the two-dimensional ambiguity function now becomes

$$P_K(t,f) \equiv \int\int A(v,\tau)K(v,\tau)e^{-2i\pi vt-2i\pi f\tau}\,dv\,d\tau .$$

This result is very important. It implies that the effect of the kernel function is that of a mask in the Doppler-lag domain of the ambiguity function. It also provides a starting point for the computation of P_K shown in Fig.1.

Before addressing the issues of interference reduction for multicomponent signals I shall present some examples of the Wigner distribution for some simple signals that will motivate the discussion on kernel design.

The first example consists of two sinusoids at frequencies of 4.5 and 9 Hz added together. The second example is a linear chirp signal extending from 2.5 Hz at a rate of 2 Hz/s. In both cases the sampling frequency is 32 Hz. These two signals (with small added random noise) are shown in Figs. 2 and 3, respectively. (All computations and images were produced using IDL from Research Systems, Inc., Boulder, CO.) Figures 4 and 5 show spectrograms of these two data sets. Notice that in Fig. 3 the frequencies are resolved quite well but the time resolution, when compared with the actual time series in Fig. 2, is quite inadequate. This trade-off between the frequency and time resolutions is, of course, the main problem with the spectrogram and the reason why other time-frequency distributions have been sought. The situation for the chirp is far worse, and the spectrogram fails miserably.

Figure 6 shows the standard Wigner distribution of the two sinusoids. Clearly, they are very well resolved both in time and frequency, but the image suffers from the cross-term "ghost" between the two frequencies. This ghost is precisely the sort of interference that we wish to minimize in the analysis of multicomponent signals, and the key is the two-dimensional Fourier transform relation between the generalized Cohen class of distributions and the two-dimensional ambiguity function. To design an
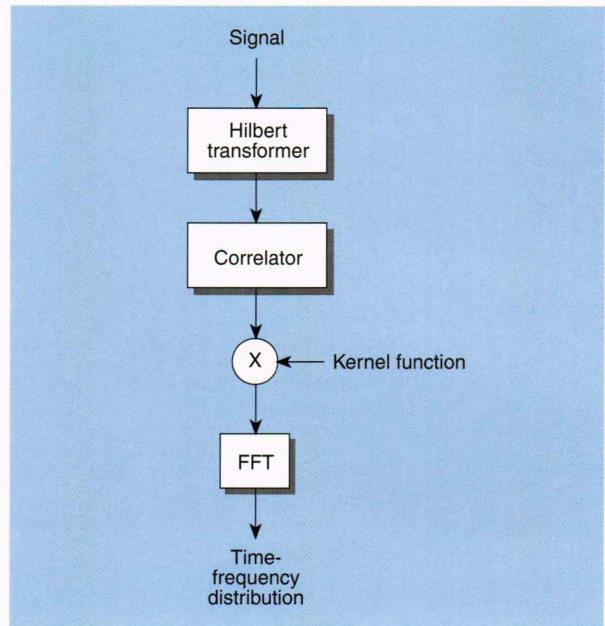

Figure 1. Computation of time-frequency distributions (FFT = fast Fourier transform).
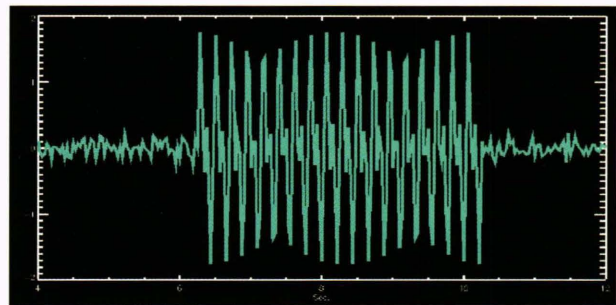

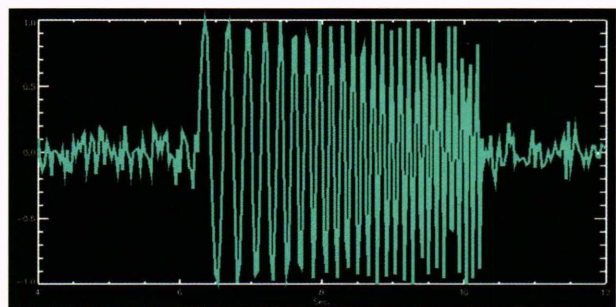**Figure 2.** Time series of two sinusoids.

Figure 3. Time series of the chirp signal.

appropriate kernel function we must look at the magnitude of the ambiguity function shown in Fig. 7. The contributions from the original frequencies lie close to the lag axes (at both ends of the Doppler axis). The design strategy for this example is now clear: the kernel function must have most of its energy concentrated along the two ends of the Doppler axis.
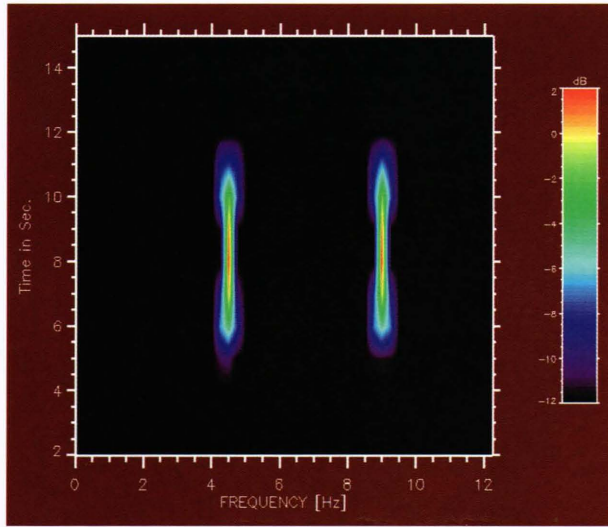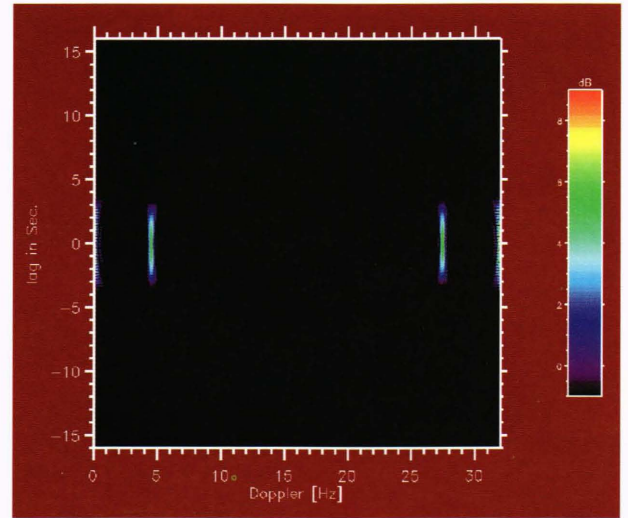
Figure 4. Spectrogram of two sinusoids.

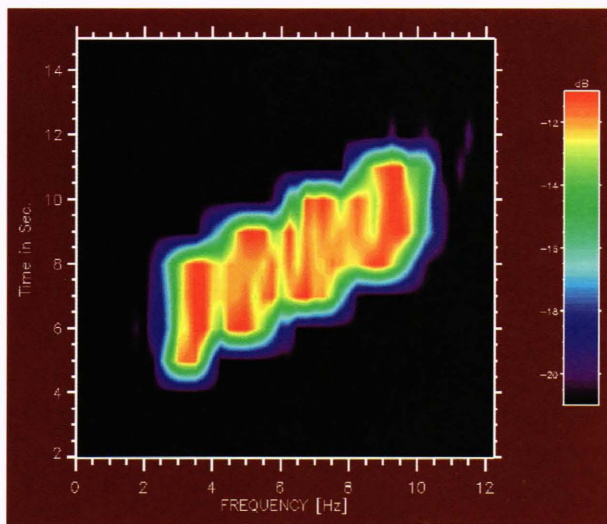**Figure 7.** Magnitude of the ambiguity function of two sinusoids.

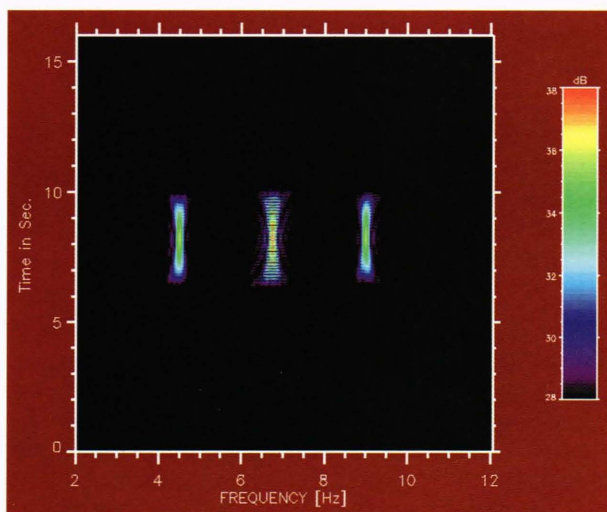**Figure 5.** Spectrogram of the chirp signal.

Figure 6. Wigner distribution of two sinusoids (kernel = 1).

Two well-known classes of kernel functions can easily be made to satisfy the preceding design criterion. The Choi–Williams[4] (CW) class is parametrized by a single parameter σ and is defined as

$$K_{CW}(v,\tau) = \exp\left(-\frac{v^2\tau^2}{\sigma}\right).$$

The Zhao–Atlas–Marks[5] (ZAM) class of kernels is of the form

$$K_{ZAM}(v,\tau) = g(t)\frac{\sin(2\pi v|\tau|/a)}{\pi v},$$

where the function $g(\tau)$ is arbitrary, and the parameter a is a number greater than or equal to 1. Generally, the function $g(\tau)$ is set equal to 1.

The CW and ZAM classes of kernel functions were originally derived based on certain mathematical conditions. For instance, the ZAM kernel was derived in the time-lag, i.e., (t, τ), domain by requiring a finite time support for the distribution, which led to the so-called cone-shaped kernels given by

$$K_{ZAM}(t,\tau) = \begin{cases} g(\tau), & |\tau| \ge a|t| \\ 0, & \text{otherwise} \end{cases}.$$

The kernel in the Doppler-lag domain is the Fourier transform of the above with respect to the time t variable, and the result is exactly the form given for K_{ZAM}. The computation of the ZAM distribution can be simplified somewhat since the defining equations reduce to

$$P_{ZAM}(K\Delta T, f) =$$

$$2(\Delta T)^2 \sum_{l=-\infty}^{l=\infty} e^{-4i\pi f l \Delta T} \sum_{m=k-2\left|\frac{l}{a}\right|}^{m=k+2\left|\frac{l}{a}\right|} \tilde{s}^*[n-l]\tilde{s}[n+l] \ .$$

Clearly, in order to reduce interference terms in a time-frequency distribution of the Cohen class of multicomponent signals, one needs an appropriate "mask" function in the Doppler-lag domain. This observation, of course, opens the door to a whole new class of experimental functions that may not lead to tractable analytic forms for the distributions but may be computationally efficient and have properties that need to be explored. One example of such a kernel function will be given later when I discuss the real data examples.

An appropriate CW kernel for the two sinusoids is shown in Fig. 8, and the corresponding CW distribution is shown in Fig. 9, in which the cross term has been successfully removed and the two sinusoids are well resolved, both in time and frequency. A similar result can be obtained using the ZAM distribution, with the ZAM parameter chosen as 1 or 2.

Figure 10 shows the ambiguity function of the chirp signal. Obviously, to resolve the chirp accurately, no mask should be used in the Doppler-lag domain. Figure 11 shows the Wigner distribution of the chirp and the excellent resolution both in time and frequency. The chirp signal is one example of a class of signals that are not multicomponent.

The important lesson of the preceding examples is that the design of the kernel function must take into account the type of signal whose time-frequency representation is sought; multicomponent signals need "narrow" kernels, whereas chirp-like signals need as wide a kernel as possible, perhaps none at all! In the next section I shall show the results of applying some of these ideas to two real data sets that were obtained by APL staff during two completely different experiments using different sensors.

APPLICATIONS TO SOME REAL DATA

The first data set is the output of an electromagnetic sensor. The time series shown in Fig. 12 consists of 3072 points sampled at 216 Hz. The purpose of the analysis is the search for some very weak harmonics of a 4-Hz signal, specifically one at 24 Hz in the first 4 s of the data. We also know that there are other frequency components
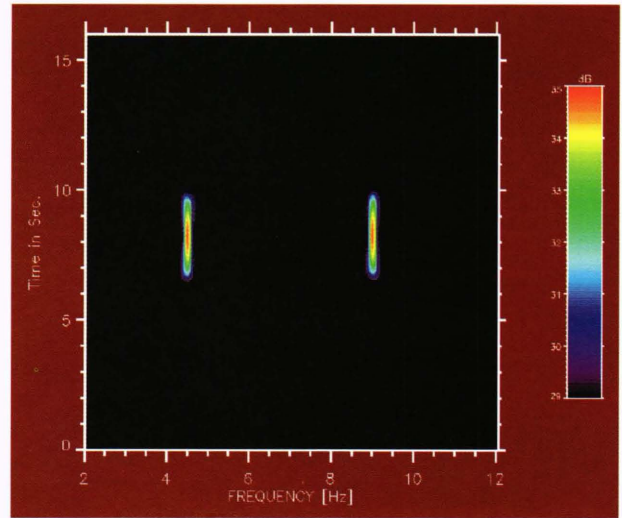

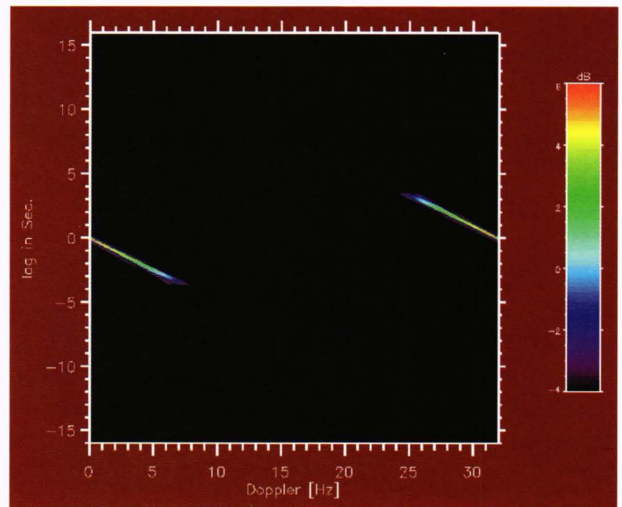**Figure 9.** Choi–Williams distribution of two sinusoids using the kernel in Fig. 8.

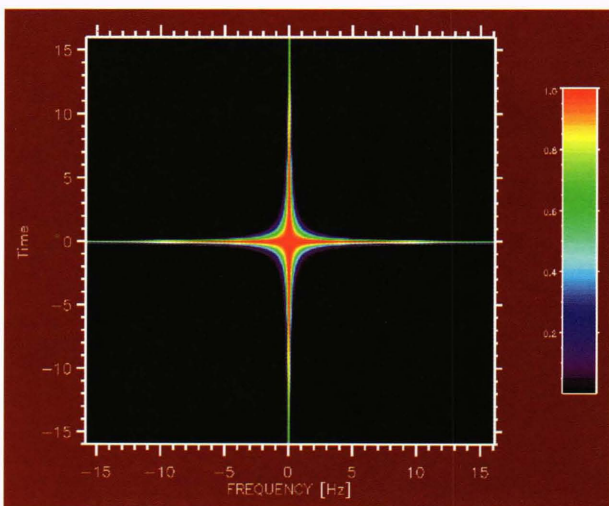**Figure 10.** Magnitude of the ambiguity function of the chirp signal.

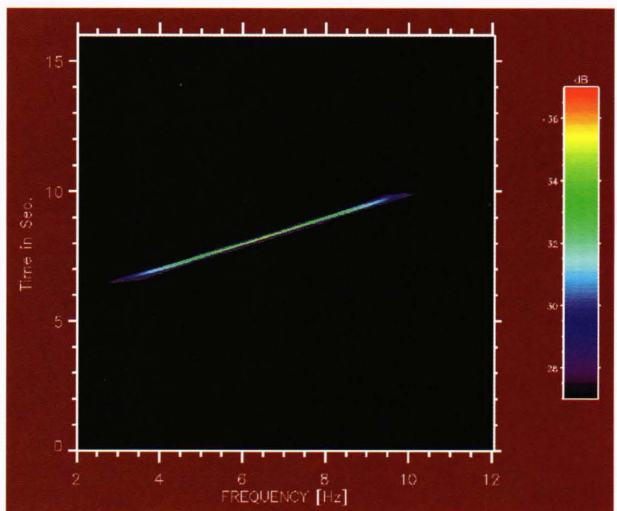**Figure 8.** Choi–Williams kernel function for two sinusoids.

Figure 11. Wigner distribution of the chirp signal (kernel = 1).

(notably, one at 25 Hz) that are not of interest but whose presence in the distribution will validate the method.

Figure 13 shows a spectrogram of this data set. There is, perhaps, a hint of the presence of the signals of interest, but not enough frequency resolution to identify the two signals. Increasing the section lengths leads to even worse results because the data length is so short. Figure 14 shows a ZAM time-frequency distribution for the first 5 s of these. A distinct component is present at 24 Hz between 3.5 to 4.5 s of the data as well as one at 36 Hz, 0.5 s before. The 25-Hz component lasts for 1 s starting at 2.5 s into the data. The ZAM distribution in this case has shown enormous improvement over the standard spectrogram.

The second data set is the output of a wave current meter deployed during an internal wave experiment.[6] The data set is 512 points long, sampled once every 6 s, and is shown in Fig. 15. Theoretical calculations for the current meter data predicted a chirp signal in the 0.002- and 0.007-Hz range 10 min into the data. In practice, interference effects caused a slow fading of the amplitude of the chirp between 0.007 and 0.008 Hz, after which the chirp was expected to be visible again. Figure 16 shows a standard spectrogram for this data set. Something remotely resembling two chirps can be seen, although the frequency and time resolutions are too poor to ascertain anything. Figure 17 shows a kernel function that I

designed specifically for this data set; although unusual, it does seems to lead to results superior to the standard Wigner distribution (i.e., unity kernel function). The resulting distribution is shown in Fig. 18, and appears to verify the theoretical expectation and offer a definite advantage over the spectrogram.
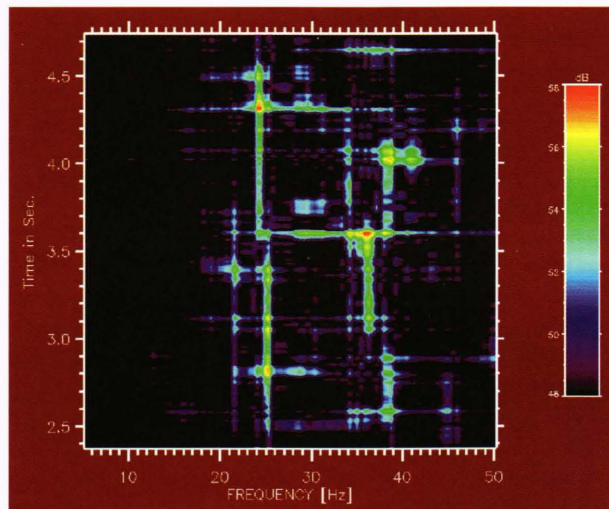

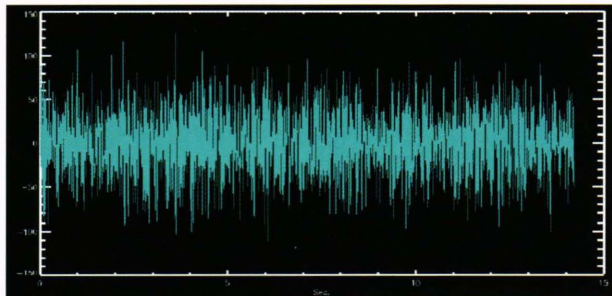**Figure 14.** Zhao–Atlas–Marks distribution of electromagnetic data.

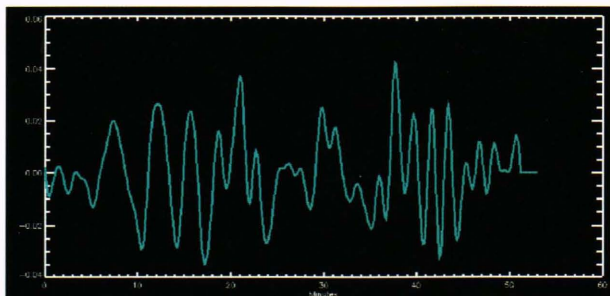**Figure 12.** Time series of electromagnetic data.
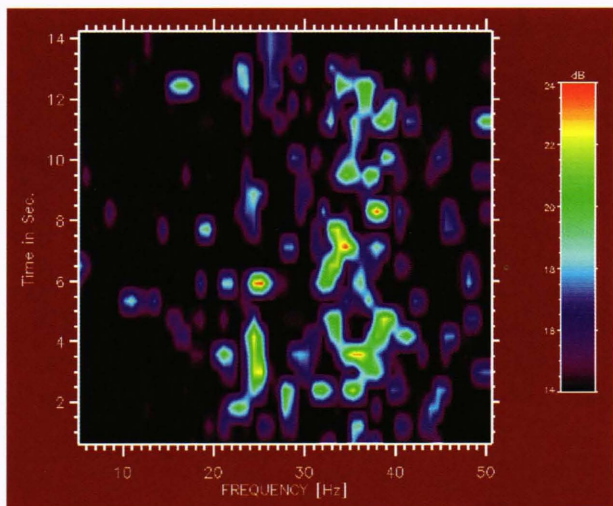

Figure 15. Time series of ocean current data.

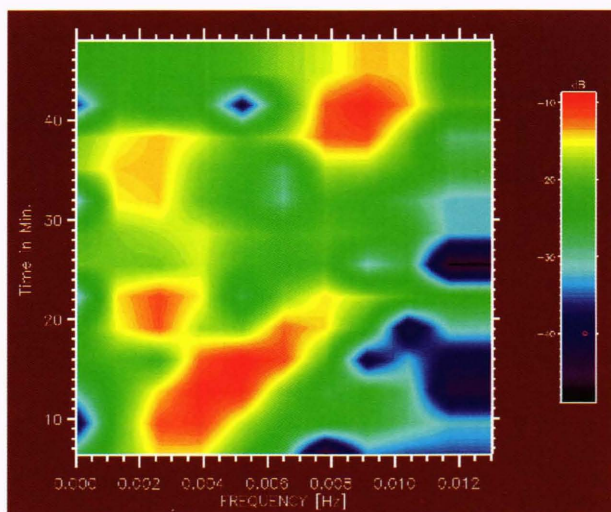**Figure 13.** Spectrogram of electromagnetic data.
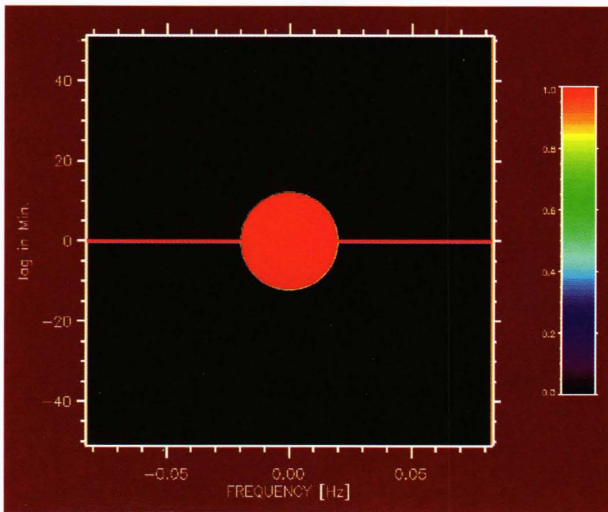

Figure 16. Spectrogram of ocean current data.

Figure 17. Experimental kernel function for ocean current data.
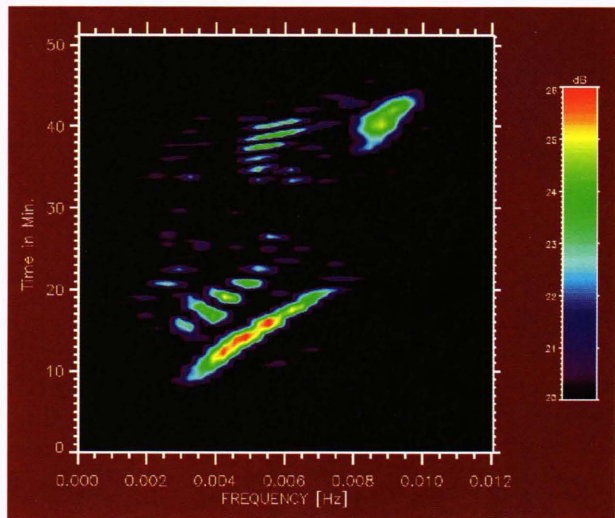

Figure 18. Wigner distribution of ocean current data using kernel in Fig. 17.

CONCLUSION

In this article I have presented the Wigner time-frequency distribution and emphasized its relationship to the two-dimensional ambiguity function. I have shown some interesting results of applying these distributions to real data sets. Time-frequency analysis is an extremely important area of signal processing, and the Wigner distribution and related functions provide us with a powerful tool in the analysis. The design of kernel functions is perhaps the most important aspect of the analysis, and the ambiguity function space of the data provides the most natural place to study such designs.

REFERENCES

[1] Boashash, B. (ed.), *Time-Frequency Signal Analysis,* Halsted Press, Melbourne, Australia (1992).
[2] Cohen, L., "Time-Frequency Distributions—A Review," *Proc. IEEE* **77**(7), 941–981 (1989).
[3] Nuttall, A. H., "Wigner Distribution Function: Relation to Short-Term Spectral Estimation, Smoothing, and Performance in Noise," in *Signal Processing Studies,* Report #8225, Naval Underwater Systems Center, New London, CT (1989).
[4] Choi, H-L., and Williams, W. J., "Improved Time-Frequency Representation of Multicomponent Signals Using Exponential Kernels," *IEEE Trans. ASSP* **37**(6), 862–871 (1989).
[5] Zhao, Y., Atlas, L. E., and Marks, R. J., "The Use of Cone-Shaped Kernels for Generalized Time-Frequency Representations of Nonstationary Signals," *IEEE Trans. ASSP* **38**(7), 1084–1091 (1990).
[6] Chapman, R., and Watson, G., *Loch Linnhe 89 Current Meter Analysis Report,* JHU/APL S1R-91U-002 (Jan 1991).

THE AUTHOR

AMIR-HOMAYOON NAJMI received B.A. and M.A. degrees in mathematics from the University of Cambridge (1977) where he completed the Mathematical Tripos, and the D.Phil. degree in theoretical physics from the Astrophysics Department of the University of Oxford (1982). He was a Fulbright scholar at the Relativity Center of the University of Texas at Austin (1977–1978), Research Associate and Instructor at the University of Utah (1982–1985), and Research Physicist at the Shell Oil Company Bellaire Geophysical Research Center in Houston (1985–1990). Dr. Najmi joined the Remote Sensing Group at APL in December 1990.